University of Groningen

Absorption of CO2 and H2S in Aqueous Alkanolamine Solutions using a Fixed-Bed Reactor with Cocurrent Downflow Operation in the Pulsing Flow Regime

Versteeg, G.F.; Swaaij, W.P.M. van

Link to publication in University of Groningen/UMCG research database

Absorption of CO_2 and H_2S in Aqueous Alkanolamine Solutions using a Fixed-Bed Reactor with Cocurrent Downflow Operation in the Pulsing Flow Regime

Absorption von CO_2 und H_2S in wäßrigen Alkanolamin-Lösungen in einem Festbettreaktor bei abwärtsfließendem Gleichstrombetrieb und pulsierendem Arbeiten

G. F. VERSTEEG and W. P. M. VAN SWAAIJ

Department of Chemical Engineering, Twente University of Technology, P.O. Box 217, 7500 AE Enschede (The Netherlands)

Abstract

Absorption rates of H_2S and CO_2 in several aqueous alkanolamines in a cocurrent downflow fixed-bed reactor operated in the pulse flow regime have been measured in order to obtain information on the potential selectivity and on the mass transfer parameters. From these experiments it can be concluded that this type of reactor seems to be very suitable for the selective removal of H_2S from acid gases.

It was not possible to derive correlations which are always valid for the calculation of the mass transfer parameters in laboratory-scale contactors. The results of the present study in combination with the data published in the literature were correlated with only one unknown parameter in which the influence of the physical properties of the system and the shape and material of the packing were combined. This parameter has to be determined empirically.

Small amounts of acid gases in aqueous alkanolamine solutions have a pronounced effect on the properties, such as the foaming behaviour, of the liquid phase. The pressure drops measured in the cocurrently operated fixed-bed reactor were affected substantially by small amounts of acid gases present in the aqueous alkanolamine solutions and up to now this effect could not be explained satisfactorily.

For the design of contactors for industrial purposes, detailed scale-up rules are required. In the present study this aspect is not investigated.

Kurzfassung

Es wurden Absorptionsraten von H_2S und CO_2 in einigen wäßrigen Alkanolaminen in einem Festbettreaktor bei abwärtsfließendem Gleichstrombetrieb und pulsierendem Arbeiten gemessen, um Informationen über die mögliche Selektivität und die Stoffübergangskoeffizienten zu erhalten. Aus diesen Experimenten kann gefolgert werden, daß dieser Reaktortyp sehr gut für die selektive Entfernung von H_2S aus sauren Gasen geeignet zu sein scheint.

Es war nicht möglich, allgemein gültige Korrelationen zur Berechnung der Stofftransportkoeffizienten in Kontaktapparaten im Labormaßstab herzuleiten. Die Ergebnisse dieser Untersuchung wurden zusammen mit den Literaturdaten korreliert, wobei ein unbekannter Parameter angepaßt werden mußte. In diesem Parameter sind die Stoffwerte des Systems sowie Form und Material der Schüttung zusammengefaßt.

Kleine Mengen saurer Gase in wäßrigen Alkanolaminlösungen haben einen starken Einfluß auf die Eigenschaften der flüssigen Phase, wie z.B. das Schäumungsverhalten. Die gemessenen Druckverluste in dem Gleichstrom-Festbettreaktor änderten sich deutlich in Anwesenheit kleiner Mengen saurer Gase in den wäßrigen Alkanolaminlösungen. Bisher konnte keine befriedigende Erklärung für diesen Effekt gefunden werden.

Für das Design industriell genutzter Kontaktapparate sind detaillierte Scale-up-Regeln erforderlich. Dieser Aspekt ist nicht Gegenstand der vorliegenden Untersuchung.

Synopse

Die Anwendung von im Gleichstrom betriebenen Festbettreaktoren zur selektiven Entfernung von H_2S aus sauren Gasen ist theoretisch von Blauwhoff et al. [2] untersucht worden. Aus dieser Untersuchung kann geschlossen werden, daß dieser Reaktortyp sehr gut für die selektive H_2S-Entfernung geeignet ist.

Aus der Literatur sind keine Korrelationen bekannt, mit denen verläßliche Stofftransportkoeffizienten und Phasenaustauschflächen für oben genannten Anwendungsfall berechnet werden können. Darüber hinaus lassen die Literaturdaten auch eine Beschreibung der Hydrodynamik (Druckverlust, Belastungsbereich) nicht zu. Daher wurde in dieser Arbeit ein Festbettreaktor, der bei abwärtsfließendem Gleichstrom betrieben wird, experimentell untersucht, um das Ergebnis der Berechnungen von Blauwhoff et al. [2] zu bestätigen und diesen Reaktortyp zu charakterisieren.

Der wesentliche Teil der Untersuchungen bestand aus der Bestimmung der volumetrischen Gas- und Flüssigkeitsstofftransportkoeffizienten k_La und k_Ga sowie der Phasengrenzfläche a. Diese drei Parameter können aus den Absorptionsraten von CO_2 und H_2S in wäßrigen Alkanolaminlösungen unter Variation von Konzentrationen und Alkanolaminen berechnet werden. Zusätzlich wurde der Druckverlust gemessen, der zur Interpretation der Absorptionsdaten (siehe Gl. (5)) benötigt wurde. Der Einfluß von Packungsart und Material wurde ebenfalls untersucht.

Während der Experimente wurde der Reaktor praktisch immer in dem Belastungsbereich betrieben, in dem er pulsierend arbeitet. Diese Ergebnisse stehen im Widerspruch zu Diagrammen über Belastungsbereiche aus der Literatur [20–22]. Die Pulsation begann am Boden der Kolonne und variierte mit den Verfahrensparametern und der Gesamtschüttungshöhe. Die Pulsation trat im gesamten Reaktor bei jeweils identischen Verfahrensparametern bei allen Packungshöhen auf.

Die Phasengrenzfläche wurde bei der Absorption von CO_2 in einer wäßrigen di-Isopropanolamin-(DIPA) Lösung bestimmt. Aus diesen Experimenten wurde eine Korrelation abgeleitet, mit der die Phasengrenzfläche für dieses System und diese Verfahrensbedingungen berechnet werden kann (Gl. (17)). Es ist möglich, die in der Literatur veröffentlichten Daten über Phasengrenzflächen mit Gl. (17) zu Korrelieren, wobei die in der Gleichung enthaltene Konstante von den physikalischen und chemischen Eigenschaften des Systems sowie von Art und Material der Packung abhängt.

Es wurde versucht, die volumetrischen Stofftransportkoeffizienten in der Gasphase, k_Ga aus der Absorption von H_2S in der gleichen DIPA-Lösung zu bestimmen, die für die Phasengrenzflächenmessung benutzt wurde. Dabei war aber für alle experimentell untersuchten Bedingungen der H_2S-Umsatz größer als 98%, sogar bei Packungshöhen von 0,04 m. Es war daher nicht möglich, genaue Informationen über den volumetrischen Stofftransport koeffizienten in der Gasphase aus der Absorption von H_2S in DIPA zu erhal-

ten. Grob abgeschätzte Werte für k_Ga liegen zwischen 15 und 140 s^{-1}.

Die volumetrischen Stofftransportkoeffizienten in der flüssigen Phase, k_La, wurden aus der Absorption von CO_2 in wäßriger MDEA-Lösung bestimmt. In dem Bereich, in dem die Hatta-Zahl zwischen 0,3 und 2 liegt, war es möglich, k_L und a beide explizit aus den Absorptionsdaten für einige spezifische experimentelle Bedingungen zu berechnen. Die so erhaltene Korrelation für die Phasengrenzfläche stimmt gut mit den Ergebnissen für das CO_2–DIPA-System und den Literaturdaten überein. Vergleicht man die Literaturangaben für k_La mit den hier gewonnenen Daten, dann zeigt sich eine bemerkenswert gute Übereinstimmung zwischen verschiedenen Autoren bezüglich des Einflusses von Gas- und Flüssigkeitsbeladung auf k_La. Der volumetrische Stofftransportkoeffizient in der Flüssigphase kann mit Gl. (21) berechnet werden. Ähnlich wie die Korrelation für die Phasengrenzfläche kann auch die für k_La nicht verallgemeinert werden. Die Konstante in Gl. (21) muß aus Experimenten mit dem System bestimmt werden, das in der praktischen Anwendung benutzt werden soll.

Der pulsierend arbeitende Gleichstrom-Festbettreaktor ist gut zur H_2S-Absorption in wäßrigen Alkanolaminlösungen geeignet, insbesondere bei niedrigen Konzentrationen in der Gasphase. Dieser Reaktortyp ist außerordentlich gut für die selektive H_2S-Entfernung geeignet, da die gleichzeitige Absorption von CO_2 stark unterdrückt wird. Dies ist auf die sehr niedrigen Packungshöhen zurückzuführen, die benötigt werden, um die erforderliche H_2S-Konzentration in der Gasphase zu erreichen.

Für die Berechnung von Phasengrenzfläche und volumetrischem Stofftransportkoeffizienten in der Flüssigkeit wurden Korrelationen aufgestellt. Die Übereinstimmung der Ergebnisse dieser Untersuchung mit Literaturdaten kann als sehr gut bezeichnet werden. Die Konstanten in den Gln. (17) und (19) hängen von den chemischen und physikalischen Eigenschaften jedes Systems sowie von Form und Material der Packung ab.

1. Introduction

The removal of the acid gas components CO_2 and H_2S from acid gas streams is often achieved by means of absorption into an aqueous alkanolamine solution. These processes are usually carried out in sieve tray columns [1] operated in a countercurrent mode. In many cases, however, only the H_2S has to be removed and particularly for these situations selective gas treatment processes are required.

The selectivity of the treatment process is determined by the mass transfer parameters of the gas–liquid contactor, the reactivity and the capacity of the solvent with respect to both CO_2 and H_2S. In the tray absorbers used traditionally, the improvement of the selectivity which can be achieved is very limited [2] and so other gas–liquid contactors have to be investigated or developed for use as a selective absorber.

Blauwhoff and van Swaaij [3] demonstrated that for an aqueous di-isopropanolamine (DIPA) solution the selectivity factor S (their eqn. (36)), which they used as a yardstick for the selectivity, increased with the ratio of the gas-phase and liquid-phase mass transfer coefficients, k_G/k_L, and therefore they concluded that a higher selectivity can be obtained by manipulation of the mass transfer parameters. A possible way to increase this ratio is the variation of both gas and liquid flows in the contactor over a wide range; this variation, however, is often restricted by the hydrodynamic limitations imposed on a stable reactor operation.

The fixed-bed reactor operated with cocurrent downflow is a well-known gas–liquid contactor which remains stable over a very wide range of hydrodynamic conditions [4]. For this contactor Blauwhoff et al. [2] studied theoretically the absorption of CO_2 and H_2S in several aqueous alkanolamine solutions and compared the selectivity calculated with the outcome of the calculations for the tray absorber. From this comparison it could be concluded that in a cocurrent downflow fixed-bed reactor a substantial increase in selectivity may be obtained.

In the open literature many papers have been published on nearly all topics concerning the application of the cocurrently operated fixed-bed reactor in chemical processes; it should be noted, however, that nearly all the experiments were carried out in laboratory-scale apparatus. Unfortunately, in spite of the large number of publications, no description which is always valid, not even for a single feature, has been established. Therefore it was not possible to obtain accurate information on the use of this reactor for gas treatment processes in general and especially for the application of selective H_2S removal processes. For the industrial application of the fixed-bed reactor in gas treatment processes reliable scale-up design rules are also necessary.

In order to obtain information on the application of this particular process the fixed-bed reactor operated with cocurrent downflow was studied in a laboratory scale for the absorption of both CO_2 and H_2S in several alkanolamine solutions. The main effort was focused on the determination of the mass transfer rates of both acid gas components. Scale-up aspects were not investigated in the present study.

2. Review

2.1. Flow map

For the fixed-bed reactor operated with cocurrent downflow, several different flow regimes can be distinguished. Firstly, the gas continuous regime with very low hydrodynamic interaction, which can be compared to the regime in a fixed bed operated in the countercurrent mode. At higher gas loadings this regime changes to spray or mist flow where a part of the liquid is transported through the reactor as very small droplets; the gas phase, however, remains the continuous phase. Secondly, at higher liquid and gas loads, liquid-rich and gas-rich waves travel alternately through the reactor and this is called the pulsing flow regime. The substantial increase in mass transfer rates and the decrease in axial mixing observed for this regime may be very advantageous. Thirdly, with increasing liquid loading the number of liquid-rich waves increases until the liquid phase becomes the continuous phase and the bubble flow regime is reached.

In order to determine the flow regime that arises when a cocurrently operated fixed-bed reactor is used, a large number of flow maps are available; these have been reviewed for non-foaming gas liquid systems by Tosun [5] and at the same time additional experimental data were presented. The flow map derived by Tosun [5] is able to correlate the data fairly well for non-foaming systems, but it is not able to account for the substantial changes in flow regime brought about by the addition of small amounts of surfactants (reported by Chou et al. [6]). Another aspect that remains to be considered is the influence of the void fraction which was not studied systematically. For foaming systems no reliable flow maps are available at present.

When aqueous alkanolamine systems, which can be regarded as moderately foaming systems, are used for gas treatment processes, several agents and defoamers in particular are added to the solvent. Therefore none of the flow maps presented so far is expected to predict accurately the flow regime which may occur during the process.

2.2. Pressure drop

The pressure drop is an important parameter in the design of gas–liquid cocurrent downflow fixed-bed reactors. For the calculation of the pressure drop two empirical approaches were favoured in the past. The first approach uses Lockhart–Martinelli parameters adapted for two-phase flow in packed beds and originally introduced by Larkins et al. [7]. The other method is the description of the pressure drop in terms of a two-phase friction factor as a function of the liquid and gas loads, as was developed by Turpin and Huntington [8]. Tosun [9] reviewed both approaches for non-foaming systems and he also presented new data. He derived a new correlation of the Lockhart–Martinelli type and the agreement is fairly good. However, to apply these correlations the single-phase pressure drops for both the gas and liquid phases are necessary and these must either be measured experimentally or estimated with the Ergun equation. As will be shown later, these types of correlations for the calculation of the pressure drop are not able to explain all observed pressure drops satisfactorily.

Rao et al. [10] developed a more fundamental approach for the calculation of the pressure drop, the geometrical interaction model, in which the influence of bubble formation on the pressure drop was

also included. This model was extended by Rao and Drinkenburg [11] especially for the pulsing flow regime and they also developed a modified geometrical interaction model for the high interaction regime [12]. Although the pressure drop measured could be predicted accurately, application of these more fundamental approaches is restricted because, for the calculation of the pressure drop, several system-specific constants need to be determined experimentally. Rao et al. [13] reviewed and correlated a large amount of experimental data but their applicability is also restricted because these correlations are different for each flow regime and, as was stated before, no generalized flow map is available yet.

2.3. Holdup

From the work of Blok et al. [14] it can be concluded that the liquid holdup in cocurrently operated packed-bed reactors depends strongly on the flow regime. Therefore, owing to the absence of a flow map which is always valid, at the moment there is no overall applicable correlation for the calculation of the liquid holdup.

Information on holdup is reviewed by Herskowitz and Smith [4] and Rao et al. [13].

2.4. Mass transfer parameters

Much effort has been invested on the determination of the mass transfer parameters and many, apparently general, valid correlations have been presented. However, at present, none of these correlations presented apply satisfactorily over a wide range of conditions. The correlations for the mass transfer parameters can be grouped in three categories.

The first group of relations describes the mass transfer parameters as a function of only gas and liquid loads and sometimes a characteristic length of the packing is included. Hirose et al. [15] presented relations for the volumetric liquid-phase mass transfer coefficient $k_L a$, and for the specific contact area a, and Blok et al. [16] for $k_L a$. The application of these correlations is restricted to chemical processes which are completely identical to the experimental system used, since the influence of the physical properties of the gas and liquid phases on the mass transfer parameters is not taken into account. Also, the influence of the shape and material of the packing is not included.

For the correlations in the second group it is assumed that the mass transfer rate can be related to the energy dissipation. Gianetto et al. [17, 18] presented correlations for $k_G a$, $k_L a$ and the specific contact area, and Reiss [19] for both volumetric gas-phase and liquid-phase mass transfer coefficients. As can be concluded from these relations, the influence of diffusivity on mass transfer is not included and, according to the mass transfer models (e.g. film model and surface renewal model), the diffusivity has a pronounced effect on mass transfer. Therefore this

kind of relation can also be used only for processes which are the same as the experimental systems.

Fukushima and Kusaka [20–22] presented dimensionless mass transfer correlations in the form

$$Sh = f^{ie}(Re_L, Re_G, Sc, We, \ldots) \tag{1}$$

which is attractive because it is based on dimensionless groups. Fukushima derived these relations from his own experimental data obtained from measurements on only one experimental system in combination with the results published in the open literature. In his fitting procedure somewhat strange dimensionless groups were introduced, like the ratio of the particle diameter to the reactor diameter,

$$(d_p/d_c)^{-p} \tag{2}$$

This group, according to Fukushima, has a substantial effect on the mass transfer parameters. This is rather peculiar because for systems with a column diameter to packing diameter ratio larger than 10 an increase of the reactor diameter usually has no influence on the mass transfer parameters, as for instance was reported by Blok et al. [16], but below this ratio a pronounced effect can usually be observed owing to wall flow. Moreover, in all the relations suggested no influence of the surface tension on the mass transfer parameters is included because it was not studied systematically. However, a substantial effect is to be expected, especially in the pulsing and dispersed bubble regimes where an important part of the contact of the gas–liquid system is established through bubbles and droplets. Overall, it may be concluded that neither of these mass transfer relations has general validity.

Simultaneously, Fukushima proposed a flow map based on the dimensionless numbers of eqn. (1).

2.5. Conclusions

It can be concluded that all the correlations presented in the literature are satisfactorily applicable to processes which are identical to the experimental system in which they were established. The stated validity of several correlations over a wide range of conditions seems to be premature. Therefore at the present stage no reliable generalizations are possible.

3. Experimental and theoretical considerations

3.1. Set-up

A schematic diagram of the experimental set-up is shown in Fig. 1. Two glass columns of inner diameter 36.2×10^{-3} m were used and the maximum packing height was 0.20 m and 0.50 m respectively. The liquid was distributed by means of an arm type of distributor which consisted of four arms and was provided with five holes of diameter 0.5×10^{-3} m ($\cong 4900$ points per m^2). Before entering the reactor the gas was passed through a fixed bed in order to ensure a uniform composition. Both gas and liquid
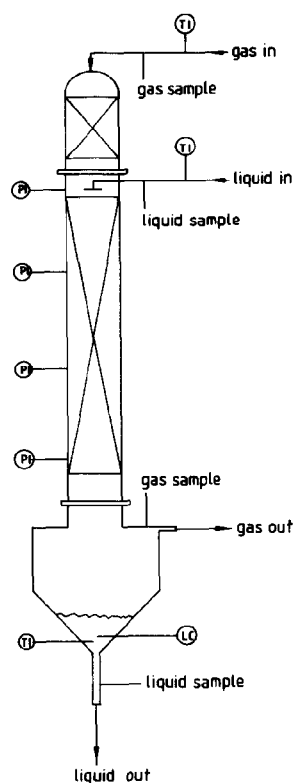
Fig. 1. Experimental set-up.

were introduced at the top of the column and were taken out from the bottom. The columns were packed randomly and in Table 1 the packing types used, together with their characteristics, are listed.

A gas–liquid separator was mounted at the bottom of the column. Several pressure taps were installed along the column to measure the pressure gradient over the whole reactor length. In the gas and liquid inlets and outlets beyond the gas–liquid separator, sample points were available at which to take samples for the determination of the composition of both phases.

The gas was saturated with water before entering the column and the flow rates were determined and kept constant with the aid of thermal mass flow controllers. The composition of the gas was analysed by means of gas chromatography. A thermal-con-

TABLE 1. Packing material specifications

Type	Material	d_p (mm)	Porosity	Geometric surface (m^{-1})
Raschig rings	Glass	4 external 2 internal	0.59	770
Spheres	Glass	3	0.39	1220
Spheres	Stainless steel	3	0.38	1240
Berl saddles	Ceramic	5.5	0.50	900

TABLE 2. Experimental systems

Amine	Concentration (mol m^{-3})	Temperature (K)	Packing
DIPA	2400	298	Glass spheres
MDEA	2010	300	Glass Raschig rings
MDEA	2010	300	Ceramic Berl saddles
MDEA	2160	300	Stainless steel spheres
MDEA	2250	300	Glass spheres

ductivity detector was used for CO_2 and a flame photometer for the extremely low H_2S concentrations ($\leqslant 500$ vol. ppm). The liquid composition was determined with standard acid–base titration for the amine concentration and the amount of acid gas absorbed by means of the method described by Jones et al. [23] and Verbrugge [24]. In an additional regeneration set-up the acid gas components in the loaded liquid were stripped off at high temperature and thus the lean liquid could be used again.

The liquid solutions were made from commercial grade amines (BASF) and distilled water. The composition and physical properties of the experimental systems used are presented in Table 2.

3.2. Theoretical aspects

The gas and liquid phases were assumed to pass through the column in plug flow. For liquid-phase and gas-phase conversions that are not too high this assumption has no effect on the outcome of the interpretation of the experiments, and it may lead to erroneous conclusions only for extremely high conversions. The material balance over a differential element of height Δx is then represented by

$$(\phi_G C_G)_x - (\phi_G C_G)_{x+\Delta x} = (\phi_L C_L)_x - (\phi_L C_L)_{x+\Delta x}$$
$$= k_{ov} a \, \Delta x (m C_G - C_{L,eq}) \quad (3)$$

with

$$k_{ov} \left(\frac{k_G}{m} + k_L E_a \right)^{-1} \quad (4)$$

This material balance cannot be solved analytically owing to the pressure gradient along the column, the decrease of the gas flow induced by the absorption of the reactive solute and the changes in the enhancement factor E_a due to the changes in the reaction rate brought about by the conversion of the amine. Therefore eqn. (3) was solved numerically.

It proved extremely difficult to take representative gas and liquid samples and so these samples were taken only at the top and the bottom of the fixed bed. The value of $k_{ov} a$ calculated from the experiments with the numerical solution of eqn. (3) includes the conversions in the entrance region of the fixed bed, the fixed-bed reactor and the gas–liquid separator. In order to obtain the correct value of $k_{ov} a$ for the fixed-bed reactor from the experiments the overall measured conversion was corrected for
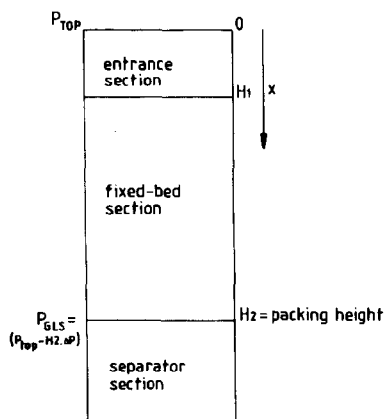
Fig. 2. Schematic representation of the reactor divided into three sections.

the contribution of the two other sections. Therefore the reactor was divided into three parts (see Fig. 2) and the following assumptions were made:

- entrance length is independent of the fixed-bed length at a given gas and liquid loading;
- the mass transfer rate in the gas–liquid separator is independent of the fixed-bed length;
- gas and liquid pass in plug flow through the entrance region and the fixed-bed section;
- the mixing in the gas–liquid separator is regarded as complete remixing;
- the pressure drop over the fixed bed can be calculated according to

$$P_x = P_{\text{top}} - \Delta P x \qquad (5)$$

With the aid of these assumptions the contributions of the three sections to the total conversion could be separated for the experiments carried out at different packing heights H_2, keeping the other experimental conditions identical. The following relation can be derived from the assumptions mentioned above:

$$mk_{\text{ov}}ad_1\left(P_{\text{top}}H_2 - \frac{H_2^{\,2}\,\Delta P}{2}\right)$$

$$= m(k_{\text{ov}}a)_{\text{entr}}d_1\ \left(P_{\text{top}}H_1 - \frac{H_1^{\,2}\Delta P}{2}\right)$$

$$+ m(k_{\text{ov}}a)_{\text{fb}}d_1\left[P_{\text{top}}(H_2 - H_1) - \frac{(H_2^{\,2} - H_1^{\,2})\,\Delta P}{2}\right]$$

$$+ \ln[1 + d_2(P_{\text{top}} - H_2\,\Delta P)] \qquad (6)$$

with

$$d_1 = \frac{M}{\phi_{\text{G, M}}RT} \qquad (7a)$$

$$d_2 = \frac{m(k_{\text{ov}}a)_{\text{GLS}}V_{\text{GLS}}MS}{\phi_{\text{G, M}}\,RT} \qquad (7b)$$

Therefore experiments were carried out for at least four packing heights in order to be able to correct

for the contributions of the entrance region and the gas–liquid separator. A relation similar to eqn. (6) was derived with the revised assumption that the gas and liquid flow in the gas–liquid separator was also plug flow; however, owing to the low conversions in this section no substantial differences in the values for $(k_{\text{ov}}a)_{\text{fb}}$ occurred.

The gas-phase mass transfer coefficient k_G is strongly influenced by the pressure of the experimental system [25] and a correction for this influence was also needed. It was assumed that the gas-phase mass transfer coefficient could be described by a dimensionless equation

$$\text{Sh}_G = \text{constant} \times (\text{Re}_L)^p(\text{Re}_G)^q(\text{Sc}_G)^r \qquad (8a)$$

with

$$\frac{k_G}{D} \propto \left(\frac{\rho v d}{\eta}\right)_G^q \left(\frac{\eta}{\rho D}\right)_G^r \qquad (8b)$$

which, for an increase in the reactor pressure, keeping the other conditions constant, leads to

$$k_G \propto P^{-1} \qquad (9)$$

independent of the values of p, q and r. Therefore the values for k_G were calculated from the experimental results and corrected to a standard pressure, $P_{\text{standard}} = 10^5$ Pa; this correction, however, is only important when the mass transfer rates are gas-phase controlled. For the verification of this assumption a systematic study of the effect of the pressure on the mass transfer parameters must be carried out.

3.3. Experimental systems

Mass transfer experiments were carried out by absorption of H_2S or CO_2 in aqueous alkanolamine solutions at temperatures between 293 K and 303 K. Aqueous solutions of DIPA and methyl diethanolamine (MDEA) were used and the physical properties determined according to Versteeg and van Swaaij [26].

The reaction between H_2S and alkanolamines can be regarded as instantaneous with respect to mass transfer [27] and for extremely low H_2S gas-phase concentrations the mass transfer rate is gas-phase controlled (see e.g. ref. 27). Therefore information on the volumetric gas-phase mass transfer coefficient k_Ga can be obtained from the absorption of very dilute H_2S into an aqueous DIPA solution.

The reaction rate of CO_2 with alkanolamines can be varied over a wide range [28, 29]. The absorption of CO_2 in aqueous alkanolamine solutions is liquid-phase controlled and therefore, depending on the choice of the amine and conditions, either k_La or a can be determined. In the present study CO_2 was absorbed in aqueous DIPA and MDEA solutions.

As the solutions were made of commercial grade amines and regenerated at high temperatures the alkanolamine solutions may be contaminated or become contaminated with small amounts of alkanolamines with a substantially different reactivity

towards CO_2. Therefore the actual reaction rate constants were determined for the solutions used at regular time intervals [28].

3.4. Correlation of the mass transfer parameters

The mass transfer parameters which were calculated from the absorption experiments according to the method described in §3.2 were correlated by means of power law expressions:

$$a/a_G = c_1(\phi_{L,M})^{c_2}(\phi_{G,M})^{c_3} \tag{10}$$

$$k_La = c_4(\phi_{L,M})^{c_5}(\phi_{G,M})^{c_6} \quad s^{-1} \tag{11}$$

and

$$k_Ga = c_7(\phi_{L,M})^{c_8}(\phi_{G,M})^{c_9} \quad s^{-1} \tag{12}$$

This way of correlating enables the present data to be compared with the results published in the literature on the possible influence of gas and liquid loadings. The influences of the physical properties of the experimental systems used, the packing shape and the material on the mass transfer parameters are located in the constants c_1, c_4 and c_7 respectively.

The effect of the reaction of CO_2 with the alkanolamine on the mass transfer rate, embodied in the enhancement factor E_a, must be taken into account. Unfortunately, it is not possible to estimate accurately the values of the mass transfer parameters which may be achieved in the fixed-bed reactor and therefore the value of E_a is also unknown. For pseudo-first-order reactions the enhancement factor can be calculated for the surface renewal theory, which seems to be the most realistic for the description of the mass transfer in the fixed-bed reactor, by [27]

$$E_a = (1 + Ha^2)^{1/2} \tag{13}$$

and

$$Ha = \frac{(k_{1,n}[amine]^n D_a)^{1/2}}{k_L} \tag{14}$$

From eqn. (13) it can easily be concluded that for low values of the Hatta number Ha (< 0.3) the value of E_a is nearly equal to unity, so that in this situation, according to eqns. (3) and (4), with the absence of any gas-phase restriction to mass transfer the volumetric liquid-phase mass transfer coefficient k_La can be measured. For larger values of Ha (> 3) the enhancement factor is about the same as the Hatta number and the specific contact area can be measured.

In the region $0.3 < Ha < 3.0$ the interpretation of the experimental results was not simple and straightforward. Since the values of the Hatta number are not known a priori, a method was developed which can be applied to interpret the results for all values of Ha when the reaction can be regarded as a pseudo-first-order reaction. For this method it was assumed that the liquid-phase mass transfer coefficient could be described by

$$k_L = c_{10}(\phi_{L,M})^{c_{11}}(\phi_{G,M})^{c_{12}} \quad m\ s^{-1} \tag{15}$$

and in combination with eqns. (10), (13) and (14) the following expression for k_LaE_a was derived:

$$k_LaE_a = a_Gc_1(\phi_{L,M})^{c_2}(\phi_{G,M})^{c_3}$$

$$\times \{[c_{10}(\phi_{L,M})^{c_{11}}(\phi_{G,M})^{c_{12}}]^2$$

$$+ k_{1,n}[amine]^n D_a\}^{1/2} \tag{16}$$

With the aid of eqn. (16) it is possible to determine k_La for low values of Ha, the interfacial area for high values of Ha, and in the intermediate region both k_L and a explicitly.

4. Results

4.1. Absorption of CO_2 in an aqueous DIPA solution

Absorption rates of CO_2 from a nitrogen stream ($\cong 10$ vol.%) in an aqueous 2400 mol m^{-3} DIPA solution were measured at 298 K in a fixed-bed reactor filled with glass spheres of diameter 3×10^{-3} m and packing heights varying between 0.060 m and 0.193 m. For this system it was expected that Ha $\geqslant 3$ and, therefore, that information on the specific contact area a could be obtained. Because the pressure drop per unit packing height is required in eqn. (6) to calculate the mass transfer parameters, this pressure drop was measured simultaneously. The experimental conditions used are presented in Table 3.

The flow regime that occurred was pulsing flow for nearly all gas and liquid loadings, and only at a liquid loading lower than 4 kg m^{-2} s^{-1} did the pulsing flow change to gas continuous. At increasing gas or liquid loadings the formation of the first pulses always started at the bottom of the reactor, which is well in line with the observations published in the literature [14]. As already mentioned in §3.2 the mass transfer parameters were determined from absorption experiments at several packing heights in order to eliminate the contributions to the conversion in the entrance region and the gas–liquid separator. However, from the experiments it appeared that for reactors with larger packing heights the transition from the gas continuous flow to the pulsing flow regime started at lower gas or liquid loadings than for reactors with short packing heights. Therefore it was observed that for a certain gas and liquid loading the reactor with a packing height of 0.060 m was still in the gas continuous region while the major part of the reactor was in the pulsing flow regime for a packing height of 0.193 m. The effect of this phenomenon on the mass transfer parameters is demonstrated qualitatively in Fig. 3 and from this Figure it

TABLE 3. Experimental conditions for the absorption of CO_2 in 2400 mol m^{-3} DIPA

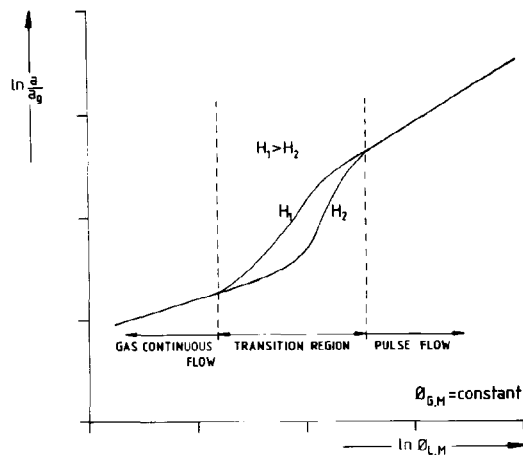| $\phi_{G,M}$ (kg m^{-2} s^{-1})	$\phi_{L,M}$ (kg m^{-2} s^{-1})	H_2 (m)	Packing
0.293–1.842	1.44–30.6	0.060–0.193	Glass spheres

Fig. 3. Effect of the transition of the flow regime on the specific contact area.

Fig. 4. Correlation of the data of the present study in the pulsing flow regime (c_4, c_5 and c_6 are 0.3, 0.32 and 0.28 kg$^{-0.60}$ m$^{1.20}$ s$^{0.60}$ respectively).

can be concluded that for the transition region these parameters cannot be determined from absorption experiments at different packing heights with the technique used at present. Therefore the start of the pulsing flow regime was defined to be when pulses were visible throughout the entire reactor, so that a unique transition boundary was obtained which only depended on the gas and liquid loading for a particular system. Only experiments in the pulsing flow regime were used to determine mass transfer parameters. The flow maps derived by Fukushima and Kusaka [20–22] were unable to predict the flow regime that arose during the experiments (see Table 4).

From the interpretation of the experiments according to eqn. (6) it could be concluded that the dimension of the entrance region was very small (less than two packing diameters) and had no effect on the determination of the desired mass transfer parameter. The contribution of the gas–liquid separator to the overall conversion ranged from about 20% up to 60% for long and short packing heights respectively. The Hatta number was always larger than 3 and therefore only the specific contact area could be determined, as was expected. The specific contact area could be described as a function of the gas and liquid loading according to eqn. (10) with
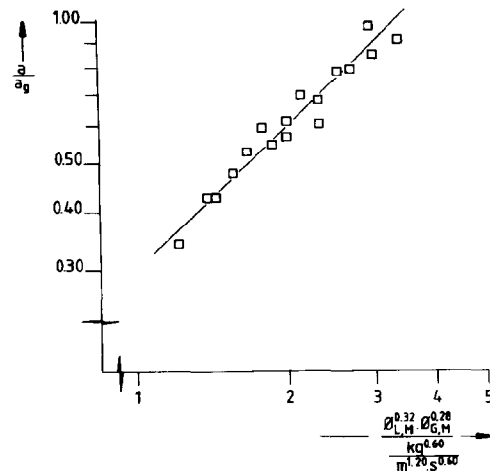
$c_1 = 0.30$ kg$^{-0.60}$ m$^{1.20}$ s$^{0.60}$, $c_2 = 0.32$ and $c_3 = 0.28$, and the average deviation between this correlation and the results is 6.3%. The experimental results are given in Table 5 and presented graphically in Fig. 4. There is considerable deviation between the specific contact areas measured and the mass transfer correlation derived by Fukushima and Kusaka [20] (see Table 4).

Gianetto et al. [18], Shende and Sharma [30], Fukushima and Kusaka [20] and Mahajani and Sharma [31] also determined the specific contact area in the pulsing flow regime. These results were re-evaluated according to eqn. (10) and in Table 6 the coefficients c_2 and c_3 are presented together with the average deviations. Only for ceramic spheres [30] and glass Raschig rings [18] do substantial differences exist between the coefficients, but it should be noted that for the latter situation experiments for only two gas loads were carried out. The coefficients presented by Mahajani and Sharma [31] are also different, which is most likely caused by the extremely small variation in both the liquid and gas loadings in their experiments. For this particular study the flow regime was mainly gas continuous and only for high loadings did the pulsing flow regime

TABLE 4. Comparison of the present results in the pulsing flow regime with the correlations of Fukushima and Kusaka

$\phi_{L,M}$ (kg m^{-2} s^{-1})	Re$_L$	$\phi_{G,M}$ (kg m^{-2} s^{-1})	Re$_G$	Flow regime (F + K)	a/a_G	
					F + K	Present study
5.04	3.50	0.297	50	Trickle	0.22	0.36
5.04	3.50	0.891	150	Spray	—	0.49
5.04	3.50	1.782	300	Spray	—	0.59
14.4	10.0	0.297	50	Trickle	0.28	0.50
14.4	10.0	0.891	150	Trickle	0.30	0.68
14.4	10.0	1.782	300	Spray	0.46	0.83
28.8	20.0	0.297	50	Trickle	0.33	0.63
28.8	20.0	0.891	150	Trickle	0.36	0.85
28.8	20.0	1.782	300	Spray	0.46	1.03

TABLE 5. Experimental results for the absorption of CO_2 in 2400 mol m^{-3} DIPA

$\phi_{G,M}$ (kg m^{-2} s^{-1})	$\phi_{L,M}$ (kg m^{-2} s^{-1})	a/a_G
0.293	5.14	0.336
0.293	8.23	0.421
0.293	12.3	0.479
0.293	20.6	0.546
0.581	5.14	0.428
0.581	8.23	0.529
0.581	14.4	0.611
0.581	22.6	0.608
1.207	5.14	0.595
1.207	9.25	0.694
1.207	15.4	0.771
1.207	24.7	0.956
1.842	5.14	0.567
1.842	8.23	0.683
1.842	13.4	0.795
1.842	18.5	0.839
1.842	26.7	0.901

arise, so restricting the variations in the loadings. The following correlation was derived from the results of the re-evaluation in combination with those obtained in the present study:

$$a/a_G = c_1(\phi_{L,M})^{0.33}(\phi_{G,M})^{0.30} \qquad (17)$$

The constant c_1 is a function of the physical properties of the system, packing shape and packing material and, unfortunately, at the present stage no further generalization was possible. The values of c_1 for the systems of Table 6 are presented in Table 7, together with the average deviations from eqn. (17). Therefore the specific contact area in a fixed-bed reactor operated with cocurrent downflow can be calculated by eqn. (17); however, the system constant c_1 must be determined experimentally for each individual system.

3.2. Absorption of H_2S in an aqueous DIPA solution

Absorption rates of H_2S from a nitrogen stream ($\cong 0.050$ vol.%) in an aqueous 2400 mol m^{-3} DIPA

TABLE 6. Re-evaluation of the results of previous investigations on a/a_G in the pulsing flow regime

$a/a_G = c_1(\phi_{L,M})^{c_2}(\phi_{G,M})^{c_3}$

Reference	c_2	c_3	Δ (%)	Packing
Gianetto et al. [18]	0.28	0.37	3.0	Glass spheres
Gianetto et al. [18]	0.26	0.30	6.8	Ceramic Raschig rings
Gianetto et al. [18]	0.20	0.18	3.0	Glass Raschig rings
Gianetto et al. [18]	0.33	0.34	4.2	Ceramic Berl saddles
Shende and Sharma [30]	0.44	0.38	3.8	Steel Pall rings
Shende and Sharma [30]	0.34	0.08	3.0	Ceramic spheres
Shende and Sharma [30]	0.37	0.22	2.3	Ceramic Raschig rings
Fukushima and Kusaka [20]	0.35	0.30	5.5	Ceramic 1/2 in. spheres
Fukushima and Kusaka [20]	0.44	0.28	10.1	Ceramic Raschig rings
Mahajani and Sharma [31]	0.60	0.52	—	Ceramic Raschig rings
Mahajani and Sharma [31]	0.87	0.32	—	Ceramic Intalox saddles

TABLE 7. Values for c_1 according to eqn. (17)

$a/a_G = c_1(\phi_{L,M})^{0.33}(\phi_{G,M})^{0.30}$

Reference	c_1 (kg$^{-0.63}$ m$^{1.26}$ s$^{0.63}$)	Δ (%)	Packing
Gianetto et al. [18]	0.42	5.7	Glass spheres
Gianetto et al. [18]	0.41	8.4	Ceramic Raschig rings
Gianetto et al. [18]	0.36	12.2	Glass Raschig rings
Gianetto et al. [18]	0.36	4.4	Ceramic Berl saddles
Shende and Sharma [30]	0.26	9.6	Steel Pall rings
Shende and Sharma [30]	0.36	17.5	Ceramic spheres
Shende and Sharma [30]	0.25	7.7	Ceramic Raschig rings
Fukushima and Kusaka [20]	0.37	5.7	Ceramic 1/2 in. spheres
Fukushima and Kusaka [20]	0.26	15.1	Ceramic Raschig rings
Mahajani and Sharma [31]	0.51	5.7	Steel Pall rings
Mahajani and Sharma [31]	0.32	10.2	Ceramic Intalox saddles
Present study	0.30	6.8	Glass spheres

solution at 298 K were measured in order to obtain information on k_Ga. The performance of the fixed-bed reactor was so good that for all experimental conditions used in the present study (see Table 8) the conversion of H_2S was greater than 98%, even at packing heights of 0.04 m. Moreover, for many experiments the chemical equilibrium between the gas phase and the loaded liquid restricted the conversion, thus having a substantial effect on the measured mass transfer rates. Therefore it was impossible to obtain accurate information on the volumetric gas-phase mass transfer coefficient k_Ga from the absorption of H_2S into an aqueous DIPA solution.

A rough estimation of k_Ga is presented in Table 9 with the assumption that the gas passes in plug flow, which may be obtained for the system mentioned above in a laboratory-scale fixed-bed reactor operated cocurrently. These values of k_Ga are of the same magnitude as those reported by Gianetto et al. [17] and Reiss [19] and substantially higher than those calculated with the relation presented by Fukushima and Kusaki [22]. For the system used in the present study, equilibrium between the gas and liquid could be approached at 50% for all experimental conditions for packing heights of about 0.05 m. This surprisingly good performance of the cocurrent fixed-bed reactor makes the design of this reactor for the selective removal of H_2S extremely simple and straightforward.

In Fig. 5 the results of the pressure drop determinations are presented graphically. The pressure drop measured for the absorption of CO_2 in DIPA is greater than that calculated according to Larkins et al. [7] and smaller than those from Sato et al. [32]; however, at the moment, no exact explanation can be presented for the substantially lower pressure drops measured for the H_2S absorption. A correlation seems to exist between the acid gas loading of the

TABLE 8. Experimental conditions for the absorption of H_2S in 2400 mol m^{-3} DIPA

$\phi_{G, M}$ (kg m^{-2} s^{-1})	$\phi_{L, M}$ (kg m^{-2} s^{-1})	H_2 (m)	Packing
0.293–1.842	5.35–27.4	0.040–0.081	Glass spheres

TABLE 9. Estimated values of k_Ga

$\phi_{G, M}$ (kg m^{-2} s^{-1})	$\phi_{L, M}$ (kg m^{-2} s^{-1})	k_Ga (s^{-1})
0.293	5.35–27.4	15–25
0.587	5.35–27.4	30–45
1.17	5.35–27.4	75–100
1.84	5.35–27.4	100–140

liquid and the pressure drop. Morsi et al. [33, 34] studied the influence of the nature of the liquid in cocurrently operated fixed beds in the gas continuous regime. He found that the liquid properties had a considerable effect on the hydrodynamics, especially on the foaming behaviour and the ionic character. None of the approaches mentioned in §2.1 for the determination of the pressure drop is able to clarify this behaviour satisfactorily. For the experiments of the present study the different acid gas loadings result in a changing ionic character of the liquid phase owing to the equilibrium composition and therefore may account for the differences in the pressure drop measured. Also it should be noted that during the absorption of CO_2 or H_2S ionic products are formed near the gas–liquid interface and these components can alter the surface tension of the liquid locally. This relative difference in the concentrations between interface and liquid bulk, which is more pronounced at low initial liquid loadings, may
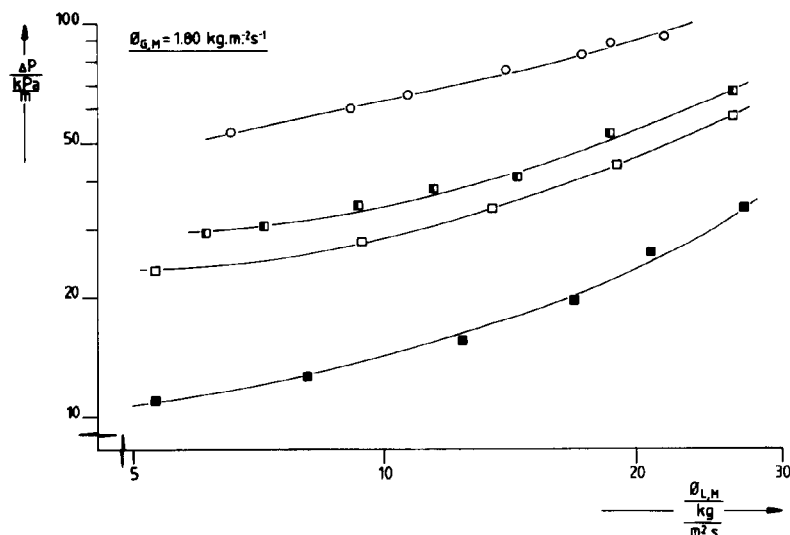

Fig. 5. Pressure drop per unit of packing height for the system with [DIPA] = 2400 mol m^{-3}: $\bigcirc$, [CO_2]$_{L, in}$ = 18.2 mol m^{-3}, $\blacksquare$, [H_2S]$_{L, in}$ = 3.53 mol m^{-3}; $\square$, [H_2S]$_{L, in}$ = 1.31 mol m^{-3}; $\blacksquare$, [H_2S]$_{L, in}$ = 0 mol m^{-3}.

also have an effect on the nature of the liquid. For instance, in our experiments carried out initially to assess information on the foaming tendency, it was observed to decrease drastically with increasing acid gas loadings.

4.3. Absorption of CO_2 in an aqueous MDEA solution

For the absorption of CO_2 from a nitrogen stream ($\cong 10$ vol.%) in an aqueous MDEA solution it was expected that the value of the Hatta number was smaller than 3 and that, depending on the value of this number, $k_L a$ or both k_L and a could be determined from the experiments. The experimental conditions used are presented in Table 10. In order to avoid excessive foaming during the absorption experiments a defoaming agent (Fluka, silicon anti-foam) was added to the solution; this may alter the physical properties of the liquid and especially the surface tension.

For this system the contribution of the entrance region to the total conversion could be neglected and the gas–liquid separator contribution ranged from 20% up to 40%, depending on the packing height. The values of the Hatta number varied between 0.30 and 2.00 and therefore both k_L and a were determined explicitly from the experiments. The specific contact area could be correlated with

$$a/a_G = c_1(\phi_{L, M})^{0.32}(\phi_{G, M})^{0.27} \tag{18}$$

The value of c_1 is presented in Table 11 and depends on both packing shape and material. The influence of both gas and liquid loading on the specific contact area is in good agreement with eqn. (17). The values of c_1 according to eqn. (17) are also given in Table 11. The liquid-phase mass transfer coefficient can be

calculated with

$$k_L = c_{10}(\phi_{L, M})^{0.54}(\phi_{G, M})^{0.04} \quad m\,s^{-1} \tag{19}$$

The value of c_{10} is presented in Table 11 and also depends on both packing shape and material. The liquid-phase volumetric mass transfer coefficient can be calculated with

$$k_L a = c_4(\phi_{L, M})^{0.86}(\phi_{G, M})^{0.31} \quad s^{-1} \tag{20}$$

The average deviations from eqn. (20) for the various packings used are given in Table 11 and the results for the stainless steel spheres and the glass Raschig rings are presented graphically in Fig. 6.

Blok et al. [16], Fukushima and Kusaka [21], Hirose et al. [15] and Gianetto et al. [17] published data on the liquid-phase volumetric mass transfer coefficient in cocurrently operated fixed-bed reactors in the pulsing flow regime. These data were re-evaluated according to eqn. (11) and the results are presented in Table 12. From this Table it can be concluded that there is remarkably good agreement between the various authors on the influence of both gas and liquid loadings on $k_L a$ and that the data from the present study are well in line with these results. Only does considerable deviation occur in the work of Hirose et al. [15], but the experiments of these authors were carried out mainly in the dispersed bubble flow regime which may cause this discrepancy. The following correlation was derived from the results of the re-evaluation in combination with those obtained in the present study:

$$k_L a = c_4(\phi_{L, M})^{0.89}(\phi_{G, M})^{0.48} \quad s^{-1} \tag{21}$$

and, identical to the situation for the correlation of the specific contact area, only a partial generalization

TABLE 10. Experimental conditions for the absorption of CO_2 in aqueous MDEA solutions

$\phi_{G, M}$ (kg m^{-2} s^{-1})	$\phi_{L, M}$ (kg m^{-2} s^{-1})	H_2 (m)	[Amine] (mol m^{-3})	Packing
0.558–2.600	11.9–31.2	0.165–0.455	2010	Glass Raschig rings
0.558–1.772	5.55–30.5	0.168–0.425	2250	Glass spheres
1.187–1.772	14.3–31.2	0.175–0.463	2010	Ceramic Berl saddles
0.558–1.187	5.64–30.8	0.162–0.548	2160	Steel spheres

TABLE 11. Values for c_1 and c_{10} according to eqns. (17), (18) and (19) and the average deviation from eqn. (20)

$a/a_G = c_1(\phi_{L, M})^{0.33}(\phi_{G, M})^{0.30}$ (17) $a/a_G = c_1(\phi_{L, M})^{0.32}(\phi_{G, M})^{0.27}$ (18)

$k_L = c_{10}(\phi_{L, M})^{0.86}(\phi_{G, M})^{0.04}$ m s^{-1} (19) $k_L a = c_4(\phi_{L, M})^{0.86}(\phi_{G, M})^{0.31}$ s^{-1} (20)

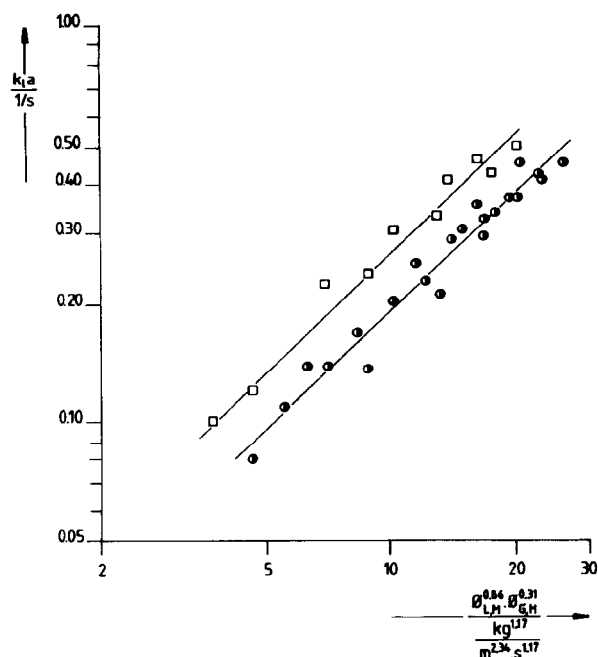| Packing	c_1(eqn. (17)) (kg$^{-0.59}$ m$^{1.18}$ s$^{0.59}$)	c_1(eqn.(18)) (kg$^{-0.59}$ m$^{1.18}$ s$^{0.59}$)	c_{10}(eqn.(19)) (kg$^{-0.58}$ m$^{2.16}$ s$^{0.41}$)	Δ (%)
Glass Raschig rings	0.72	0.68	3.8×10^{-5}	10.3
Glass spheres	0.67	0.60	3.2×10^{-5}	10.3
Steel spheres	0.66	0.61	3.6×10^{-5}	8.7
Ceramic Berl saddles	0.48	0.48	3.8×10^{-5}	7.6

Fig. 6. Correlation of the data from the present study in the pulsing flow regime: □, stainless steel spheres, $c_4 = 2.74 \times 10^{-2}\,kg^{-1.17}\,m^{2.34}\,s^{2.17}$; ◑, glass Raschig rings, $c_4 = 1.96 \times 10^{-2}\,kg^{-1.17}\,m^{2.34}\,s^{2.17}$.

is possible for $k_L a$ at the moment and the constant c_4 has to be determined from experiments carried out for the system which will be used for the practical application. The constant c_4 and the average deviation of eqn. (21) are presented in Table 13 together with the results of the present study.

5. Conclusions

The fixed-bed reactor operated cocurrently in the pulsing flow regime has an outstanding performance

for the absorption of H_2S in aqueous alkanolamine solutions, especially at low gas-phase concentrations. Very high conversions of the H_2S concentrations were obtained, even at extremely short packing heights, and the optimal packing height for practical applications will be determined mainly by the equilibrium between gas and liquid. This reactor is extremely well suited for the selective removal of H_2S because the co-absorption of CO_2 will be depressed substantially owing to the very short packing heights needed to fulfil the specification of the H_2S gas-phase concentration. However, it should be borne in mind that the CO_2 loading of the liquid has a pronounced effect on the equilibrium composition [35] and therefore may affect the required packing height.

The specific contact area a for this reactor in the pulsing flow regime can be calculated with

$$a/a_G = c_1(\phi_{L,M})^{0.33}(\phi_{G,M})^{0.30} \qquad (17)$$

and the volumetric mass transfer coefficient $k_L a$ from

$$k_L a = c_4(\phi_{L,M})^{0.89}(\phi_{G,M})^{0.48} \qquad s^{-1} \qquad (21)$$

The constants c_1 and c_4 must be determined for each process separately because the influence of the liquid-phase and gas-phase properties, packing shape and material, and also the mass transfer model which describes the mass transfer (influence of diffusivity) in this particular reactor are combined in these constants. A further generalization is not possible at the moment.

When absorption experiments are carried out for a typical system and the Hatta number can be varied from 0.3 up to 3, both the specific contact area and the liquid-phase mass transfer coefficient can be determined explicitly for one experimental system.

Passing from the gas continuous regime to the pulsing flow regime a transition region is encountered in which both regimes occur in the reactor. In the present work, pulsing flow was defined as the situation in which pulses occur throughout the whole column.

TABLE 12. Results of the re-evaluation of previous investigations on $k_L a$ in the pulsing flow regime

$k_L a = c_4(\phi_{L,M})^{c_5}(\phi_{G,M})^{c_6} \qquad s^{-1}$

Reference	c_5	c_6	Δ (%)	Packing
Gianetto et al. [17]	0.93	0.53	5.9	Glass spheres
Gianetto et al. [17]	0.85	0.43	5.5	Ceramic Raschig rings
Gianetto et al. [17]	0.89	0.32	4.7	Ceramic Berl saddles
Hirose et al. [15]	0.60	0.60	—	Glass spheres
Fukushima and Kusaka [21]	0.70	0.41	9.2	Ceramic spheres
Fukushima and Kusaka [21]	0.86	0.41	9.3	Ceramic spheres
Blok et al. [16]	0.87	0.49	8.8	Glass 0.0025 m Raschig rings
Blok et al. [16]	0.97	0.62	11.5	Glass 0.0025 m Raschig rings
Blok et al. [16]	0.91	0.55	10.5	Glass 0.0040 m Raschig rings
Blok et al. [16]	1.06	0.59	8.5	Glass 0.0040 m Raschig rings
Present study	0.86	0.31	10.3	Glass Raschig rings
Present study	0.86	0.31	10.3	Glass spheres
Present study	0.86	0.31	8.7	Steel spheres
Present study	0.86	0.31	7.6	Ceramic Berl saddle

TABLE 13. Values for c_4 according to eqn. (21)

$$k_L a = c_4 (\phi_{L,M})^{0.89} (\phi_{G,M})^{0.48} \quad s^{-1}$$

Reference	$10^2 \times c_4$ $(kg^{-1.37} m^{3.74} s^{0.37})$	Δ (%)	Packing
Gianetto *et al.* [17]	1.74	7.3	Glass spheres
Gianetto *et al.* [17]	2.01	6.2	Ceramic Raschig rings
Gianetto *et al.* [17]	1.26	13.4	Glass spheres
Gianetto *et al.* [17]	1.39	8.1	Ceramic Berl saddles
Fukushima and Kusaka [21]	1.51	5.3	Ceramic spheres
Fukushima and Kusaka [21]	0.83	10.8	Ceramic Raschig rings
Blok *et al.* [16]	2.89	8.6	Glass 0.0025 m Raschig rings
Blok *et al.* [16]	3.56	16.5	Glass 0.0025 m Raschig rings
Blok *et al.* [16]	1.45	15.8	Glass 0.0040 m Raschig rings
Blok *et al.* [16]	1.33	12.2	Glass 0.0040 m Raschig rings
Present study	1.63	12.1	Glass Raschig rings
Present study	1.87	14.3	Glass spheres
Present study	2.44	12.5	Steel spheres
Present study	1.29	9.2	Ceramic Berl saddles

Acknowledgements

Nomenclature

a	specific contact, m^{-1}
a_G	geometric contact area, m^{-1}
C	concentration, mol m^{-3}
c_1	constant defined by eqn. (10), $kg^{-(c_2+c_3)} m^{2(c_2+c_3)} s^{(c_2+c_3)}$
c_2	constant defined by eqn. (10)
c_3	constant defined by eqn. (10)
c_4	constant defined by eqn. (11), $kg^{-(c_5+c_6)} m^{2(c_5+c_6)} s^{(c_5+c_6-1)}$
c_5	constant defined by eqn. (11)
c_6	constant defined by eqn. (11)
c_7	constant defined by eqn. (12), $kg^{-(c_8+c_9)} m^{2(c_8+c_9)} s^{(c_8+c_9-1)}$
c_8	constant defined by eqn. (12)
c_9	constant defined by eqn. (12)
c_{10}	constant defined by eqn. (15), $kg^{-(c_{11}+c_{12})} m^{2(c_{11}+c_{12}+0.50)} s^{(c_{11}+c_{12}-1)}$
c_{11}	constant defined by eqn. (15)
c_{12}	constant defined by eqn. (15)
D	diffusion coefficient, $m^2 s^{-1}$
d_c	reactor diameter, m
d_p	packing diameter, m
d_1	constant defined by eqn. (7a)
d_2	constant defined by eqn. (7b)
E	enhancement factor
H_1	length of entrance region, m

H_2	packing height, m
Ha	Hatta number, defined by eqn. (14)
k_G	gas-phase mass transfer coefficient, m s^{-1}
$k_G a$	gas-phase volumetric mass transfer coefficient, s^{-1}
k_L	liquid-phase mass transfer coefficient, m s^{-1}
$k_L a$	liquid-phase volumetric mass transfer coefficient, s^{-1}
$k_{1,n}$	reaction rate constant, $m^{3n} mol^{-n} s^{-1}$
k_{ov}	overall mass transfer coefficient, defined by eqn. (4), m s^{-1}
M	molecular weight, kg mol^{-1}
m	dimensionless solubility, defined by C_L/C_G, mol mol^{-1}
P	pressure, Pa
ΔP	pressure drop per unit length, Pa m^{-1}
R	$= 8.3143$ J mol^{-1} K^{-1}, gas constant
Re	Reynolds number
S	cross-sectional area of fixed bed, m^2
Sc	Schmidt number
Sh	Sherwood number
T	temperature, K
V	volume, m^3
v	
We	Weber number
x	distance, m
ε	void fraction
η	viscosity
ρ	density, kg m^{-3}
ϕ	flow per unit cross-sectional area, $m^3 m^{-2} s^{-1}$
ϕ_m	mass flow per unit cross-sectional area, kg m^{-2} s^{-1}
[ ]	concentration, mol m^{-3}

Superscripts

p, q, r	constants

176

References

1. A. L. Kohl and F. C. Riesenfeld, *Gas Purification*, Gulf, Houston, TX, 1979.
2. P. M. M. Blauwhoff, B. Kamphuis, W. P. M. van Swaaij and K. R. Westerterp, Absorber design in sour natural gas treatment plants: impact of process variables on operation and economics, *Chem. Eng. Process.*, *19* (1985) 1–25.
3. P. M. M. Blauwhoff and W. P. M. van Swaaij, Simultaneous mass transfer of H_2S and CO_2 with complex chemical reactions in an aqueous di-isopropanolamine solution, *Chem. Eng. Process.*, *19* (1985) 67–83.
4. M. Herskowitz and J. M. Smith, Trickle-bed reactors: a review, *AIChE J.*, *29* (1983) 1–18.
5. G. Tosun, A study of cocurrent downflow of nonfoaming gas–liquid systems in a packed bed. 1. Flow regimes: search for a generalized flow map, *Ind. Eng. Chem., Process Des. Dev.*, *23* (1985) 29–35.
6. T. S. Chou, F. L. Worley and D. Luss, Transition to pulsed flow in mixed-phase cocurrent downflow through a fixed bed, *Ind. Eng. Chem., Process Des. Dev.*, *16* (1977) 424–427.
7. R. P. Larkins, R. R. White and D. W. Jeffrey, Two-phase cocurrent flow in packed beds, *AIChE J.*, *7* (1961) 231–239.
8. J. L. Turpin and R. L. Huntington, Prediction of pressure drop for two-phase, two-component cocurrent flow in packed beds, *AIChE J.*, *13* (1967) 1196–1202.
9. G. Tosun, A study of cocurrent downflow of nonfoaming gas–liquid systems in a packed bed. 2. Pressure drop: search for a correlation, *Ind. Eng. Chem., Process Des. Dev.*, *23* (1984) 35–39.
10. V. G. Rao, S. Ananth and Y. B. G. Varma, Hydrodynamics of two-phase cocurrent downflow through packed beds. Part 1: Macroscopic model, *AIChE J.*, *29* (1983) 467–473.
11. V. G. Rao and A. A. H. Drinkenburg, Pressure drop and hydrodynamic properties of pulses in two-phase gas–liquid downflow through packed columns, *Can. J. Chem. Eng.*, *61* (1983) 158–167.
12. V. G. Rao and A. A. H. Drinkenburg, A model for pressure drop in two-phase gas–liquid downflow through packed columns, *AIChE. J.*, *31* (1985) 1010–1018.
13. V. G. Rao, S. Ananth and Y. B. G. Varma, Hydrodynamics of two-phase cocurrent downflow through packed beds. Part 2: Experiment and correlations, *AIChE J.*, *29* (1983) 473–483.
14. J. R. Blok, J. Varkevisser and A. A. H. Drinkenburg, Transition to pulsing flow, holdup and pressure drop in packed columns with cocurrent gas–liquid downflow, *Chem. Eng. Sci.*, *38* (1983) 687–699.
15. T. Hirose, M. Toda and Y. Sato, Liquid phase mass transfer in packed bed reactor with cocurrent gas–liquid downflow, *J. Chem. Eng. Jpn.*, *7* (1974) 187–192.
16. J. R. Blok, C. E. Koning and A. A. H. Drinkenburg, Gas–liquid mass transfer in fixed-bed reactors with cocurrent downflow operating in the pulsing flow regimes, *AIChE J.*, *30* (1984) 393–401.
17. A. Gianetto, G. Baldi and V. Specchia, Absorption in packed towers with cocurrent downward high-velocity flows. 2—Mass transfer, *AIChE J.*, *19* (1973) 916–922.
18. A. Gianetto, G. Baldi and V. Specchia, Absorption in packed towers with cocurrent downward high-velocity flows. 1—Interfacial areas, *Ing. Chim. (Milan)*, *6* (1970) 125–133.
19. L. P. Reiss, Cocurrent gas–liquid contacting in packed columns, *Ind. Eng. Chem., Process Des. Dev.*, *6* (1967) 486–499.
20. S. Fukushima and K. Kusaka, Interfacial area and boundary of the hydrodynamic flow region in packed column with cocurrent downward flow, *J. Chem. Eng. Jpn.*, *10* (1977) 461–467.
21. S. Fukushima and K. Kusaka, Liquid-phase volumetric and mass-transfer coefficient, and boundary of the hydrodynamic flow region in packed column with cocurrent downward flow, *J. Chem. Eng. Jpn.*, *10* (1977) 467–473.
22. S. Fukushima and K. Kusaka, Boundary of hydrodynamic flow region and gas-phase mass-transfer coefficient in packed column with cocurrent downward flow, *J. Chem. Eng. Jpn.*, *11* (1978) 241–244.
23. R. F. Jones, P. Gale, P. Hopkins and L. N. Powell, A simple and rapid titrimetric method for the determination of carbon in iron steel, *Analyst*, *90* (1965) 623–629.
24. P. Verbrugge, *Ph.D. Thesis*, Delft Univ., 1979.
25. G. F. Versteeg, P. M. M. Blauwhoff and W. P. M. van Swaaij, The effect of diffusivity on gas–liquid mass transfer in stirred vessels. Experiments at atmospheric and elevated pressures, *Chem. Eng. Sci.*, *42* (1987) 1103–1119.
26. G. F. Versteeg and W. P. M. van Swaaij, The solubility and diffusivity of acid gas components in aqueous alkanolamine solutions, *J. Chem. Eng. Data*, *32* (1988) 29–34.
27. P. V. Danckwerts, *Gas–Liquid Reactions*, McGraw-Hill, London, 1970.
28. G. F. Versteeg and W. P. M. van Swaaij, On the kinetics between CO_2 and alkanolamines both in aqueous and non-aqueous solutions. Part 1: Primary and secondary amines, *Chem. Eng. Sci.*, *43* (1988) 573–585.
29. G. F. Versteeg and W. P. M. van Swaaij, On the kinetics between CO_2 and alkanolamines both in aqueous and non-aqueous solutions, Part 2: Tertiary amines, *Chem. Eng. Sci.*, *43* (1988) 587–591.
30. B. W. Shende and M. M. Sharma, Mass transfer in packed columns: cocurrent operation, *Chem. Eng. Sci.*, *29* (1974) 1763–1772.
31. V. V. Mahajani and M. M. Sharma, Mass transfer in packed columns: co-current (downflow) operation: 1 in. and 1.5 in. metal Pall rings and ceramic Intalox saddles: multifilament gauze packings in 20 cm and 38 cm i.d. columns, *Chem. Eng. Sci.*, *35* (1980) 941–947.
32. Y. Sato, T. Hirose, F. Takahashi and M. Toda, Pressure loss and liquid holdup in packed bed reactor with cocurrent gas–liquid downflow, *J. Chem. Eng. Jpn.*, *6* (1973) 147–152.
33. B. I. Morsi, A. Laurent, N. Midoux and J. C. Charpentier, Interfacial area in trickle-bed reactors: comparison between ionic and organic liquids and between Raschig rings and small diameter particles, *Chem. Eng. Sci.*, *35* (1980) 1470–1473.
34. B. I. Morsi, A. Laurent, N. Midoux and J. C. Charpentier, Hydrodynamics and interfacial areas on downward cocurrent gas–liquid flow through fixed beds. Influence of the nature of the liquid, *Int. Chem. Eng.*, *22* (1982) 142–151.
35. P. M. M. Blauwhoff and W. P. M. van Swaaij, Gas–liquid equilibria between H_2S, CO_2 and aqueous amine solutions, *Proc. 2nd Int. Conf. on Phase Equilibria and Fluid Properties in the Chemical Industry*, EFCE Publ. 11, Berlin, 1980, p. 78.